2016

Triticum mosaic virus exhibits limited population variation yet shows evidence of parallel evolution after replicated serial passage in wheat

Melissa S. Bartels
University of Nebraska-Lincoln, blackmare08@yahoo.com

Roy French
University of Nebraska-Lincoln, Roy.French@ars.usda.gov

Robert A. Graybosch
USDA-ARS, bob.graybosch@ars.usda.gov

Satyanarayana Tatineni
USDA-ARS, Satyanarayana.Tatineni@ars.usda.gov

Follow this and additional works at: http://digitalcommons.unl.edu/plantpathpapers

Part of the Other Plant Sciences Commons, Plant Biology Commons, and the Plant Pathology Commons

Triticum mosaic virus exhibits limited population variation yet shows evidence of parallel evolution after replicated serial passage in wheat

Melissa Bartels [a,b,1], Roy French [a,b,*], Robert A. Graybosch [a,c], Satyanarayana Tatineni [a,b,*]

[a] *United States Department of Agriculture-Agricultural Research Service (USDA-ARS), University of Nebraska-Lincoln, Lincoln, NE 68583, USA*
[b] *Department of Plant Pathology, University of Nebraska-Lincoln, Lincoln, NE 68583, USA*
[c] *Department of Agronomy and Horticulture, University of Nebraska-Lincoln, Lincoln, NE 68583, USA*

ARTICLE INFO

ABSTRACT

An infectious cDNA clone of *Triticum mosaic virus* (TriMV) (genus *Poacevirus*; family *Potyviridae*) was used to establish three independent lineages in wheat to examine intra-host population diversity levels within protein 1 (P1) and coat protein (CP) cistrons over time. Genetic variation was assessed at passages 9, 18 and 24 by single-strand conformation polymorphism, followed by nucleotide sequencing. The founding P1 region genotype was retained at high frequencies in most lineage/passage populations, while the founding CP genotype disappeared after passage 18 in two lineages. We found that rare TriMV genotypes were present only transiently and lineages followed independent evolutionary trajectories, suggesting that genetic drift dominates TriMV evolution. These results further suggest that experimental populations of TriMV exhibit lower mutant frequencies than that of *Wheat streak mosaic virus* (genus *Tritimovirus*; family *Potyviridae*) in wheat. Nevertheless, there was evidence for parallel evolution at a synonymous site in the TriMV CP cistron.

Published by Elsevier Inc.

1. Introduction

RNA viruses possess the characteristic features of high mutation rate, short replication cycle, and a particularly large population size, all of which can influence viral evolutionary rates (Duffy et al., 2008). The high mutation rate is attributed to the error rate of RNA-dependent RNA polymerases, a consequence of lack of proof-reading capability (Drake, 1993; Drake and Holland, 1999). Thus, RNA viruses can undergo rapid evolutionary changes and increase the population genetic diversity (Holland et al., 1982). However, low levels of variation have been observed for many plant RNA viruses indicating that accumulation of significant differences in virus populations is a slow process (Albiach-Martí et al., 2000; French and Stenger, 2005; García-Arenal et al., 2003; Kong et al., 2000; Kurath and Palukaitis, 1990). Possible reasons for this are genetic bottlenecks and negative selection (Acosta-Leal et al., 2011; French and Stenger, 2005; García-Arenal et al., 2003; Hall et al., 2001b; Li and Roossinck, 2004; Novella et al., 1995; Rodriguez-Cerezo et al., 1991). There have been a number of

studies demonstrating that population bottlenecks result in extremely low effective population sizes (French and Stenger, 2003; Li and Roossinck, 2004; Miyashita and Kishino, 2010; Miyashita et al., 2015; Sacristán et al., 2003). As a result, there is a tremendous disparity (many orders of magnitude) between effective population sizes and actual population sizes for plant viruses.

Luria (1951) proposed two plausible models of how viruses might replicate. One was an exponential growth model where mutants can multiply following the actual mutational event. Thus, the total number of mutants in a culture will vary widely depending whether the mutation occurred earlier or later in the intracellular replication cycle. The second was a linear growth model where a template is repeatedly copied as by a "stamping machine" to produce progeny viral genomes, a constant proportion of which will be mutants (see Combe and Sanjuán (2014), Duffy et al. (2008), and Safari and Roossinck (2014) for graphical representations of the two replication models and their effects on the rate at which mutations accumulate within an infected cell). There is ample evidence that positive-sense single-stranded RNA virus intracellular replication is largely linear (French and Stenger, 2003; Sanjuán et al., 2010; Sardanyés and Elena, 2011). In particular, a recent study with the positive-sense single-stranded RNA bacteriophage Qβ (García-Villada and Drake, 2012) conclusively reveals its linear mode of replication and provides an interesting

contrast to the exponential growth model of the DNA bacteriophage used in Luria's (1951) experiments.

There is also evidence that the fidelity of RNA viral replication may vary from virus to virus and host to host (Schneider and Roossinck, 2000, 2001). The interplay among variable error rates, low effective population size, very large actual population size, and linear replication and their effects on plant virus population diversity are not fully understood, both from experimental and theoretical standpoints.

Triticum mosaic virus (TriMV) is a recently described RNA virus infecting wheat (*Triticum aestivum* L). TriMV is transmitted by the wheat curl mite, *Aceria tosichella* Keifer, (McMechan et al., 2014; Seifers et al., 2009) and is wide spread in the Great Plains region of the USA (Burrows et al., 2009; Byamukama et al., 2013; Seifers et al., 2008). TriMV is the type member of the genus *Poacevirus* within the family *Potyviridae* (Fellers et al., 2009; Seifers et al., 2008; Tatineni et al., 2009). TriMV is a positive-sense single-stranded RNA virus, consisting of 10,266 nucleotides (nts) excluding the poly A tail (Fellers et al., 2009; Tatineni et al., 2009). The genome is translated into a single polyprotein that is cleaved into at least 10 mature proteins by three putative viral proteinases (P1, HC-Pro, and NIa-Pro) (Tatineni et al., 2009). The protein 1 (P1) of TriMV functions as an RNA silencing suppressor and enhancer of pathogenicity (Tatineni et al., 2012) and coat protein (CP) is required for virion assembly. However, the functions of other TriMV-encoded proteins are not known. Studies with a limited number of field-collected TriMV isolates from the Great Plains region found they were mainly homogeneous, with little sequence variation (Fuentes-Bueno et al., 2011; Seifers et al., 2013).

Wheat streak mosaic virus (WSMV) is another wheat-infecting potyvirid species (Stenger et al., 1998). WSMV and TriMV share a number of common hosts (Tatineni et al., 2010) and have the same mite vector (Slykhuis, 1955). Several aspects of population structure and evolution of WSMV have been extensively studied (Choi et al., 2001; French and Stenger, 2003; Hall et al., 2001a, b; Stenger et al., 2002). Thus, it was of interest to compare the population dynamics of the two viruses. To this end, we used single-strand conformation polymorphism (SSCP) analysis, followed by nucleotide sequencing to initiate studies on the diversities of the TriMV P1 and CP cistrons following serial passage in wheat.

We report here that three replicated passages of TriMV followed independent evolutionary trajectories but all populations were characterized by low genetic diversities. The number of mutations observed per nucleotide sequenced (mutation frequency) is also presented. Nonetheless, there was also evidence of parallel evolution in the TriMV CP cistron.

2. Results

Progeny virus from an infectious cDNA clone of a Nebraska isolate of TriMV (Tatineni et al., 2015) was used as the founding inoculum to establish three lineages, or replicate serial transmission populations (designated I, II, and III) in wheat by mechanical inoculation. Single infected plants were arbitrarily chosen from each passage to establish the next passage population. Replicate populations were sampled at passages 9, 18, and 24. RNA was extracted from each sample and reverse transcribed using gene-specific primers. The cDNA was amplified by PCR using two primer sets. One set amplified a region spanning nts 301–1888 of the TriMV genome (P1 region) and the other amplified a region spanning nts 9001–10,078 (CP region) (Fig. 1). The P1 region contains a portion of the 5′UTR (nts 301–739) extending to the end of the P1 cistron, while the CP region contains part of the NIb cistron (nts 9001–9193) followed by the complete CP cistron (Fig. 1).

2.1. Phenotypic analysis of cDNA clones

PCR products were inserted into a cloning vector and 20 clones from each genomic region, lineage, and passage were selected for analysis (360 clones in total). These were then analyzed by SSCP (Fig. 2) that allows ready assessment of the structure and diversity within and between populations. We use the term phenotype to describe SSCP pattern variants because, while differences among SSCP patterns are certainly due to nucleotide sequence variation, the extent of such differences is unknown.

Phenotypes were labeled in either uppercase (P1 region) or lowercase (CP region) letters (Table 1), where 'A' and 'a' indicate the phenotype of the P1 and CP regions of the parental cDNA clone used as the initial inoculum. There were 28 variants among the P1 region clones and 34 variants among the CP region clones. Variability in the number of phenotypes was evident among all population samples, ranging from a minimum of two to a maximum of eight. Gene identity (homozygosity) values provide a summary statistic to quantify this variation and allow ready comparisons among populations. Essentially, gene identities represent the probability that any two clones derived from the same population have identical phenotypes. These values ranged from 0.232 to 0.900 (Table 1). There were no significant differences ($P=0.91$) among gene diversities of the nine replicate/passage populations. Thus, no clear trends were observed between genomic regions or among replicates or passages.

As each clone represents an individual drawn from a very large total cDNA population, these experiments can be viewed as a series of binomial trials. As can be seen with the binomial probabilities tabulated in Table 2, unique phenotypes can only be
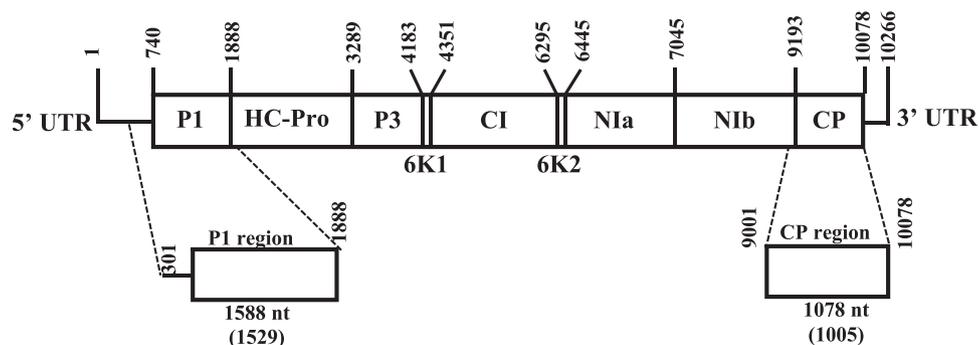
Fig. 1. Schematic representation of the TriMV genome. Location of cistrons in the TriMV genome is indicated in the open reading frame encoding for the polyprotein. The 5′ and 3′ untranslated regions (UTR) are indicated. Below are presented the fragments amplified by RT-PCR with its size and in parentheses the number of nucleotides analyzed to determine the nucleotide polymorphism of each analyzed region.

20°C   4°C
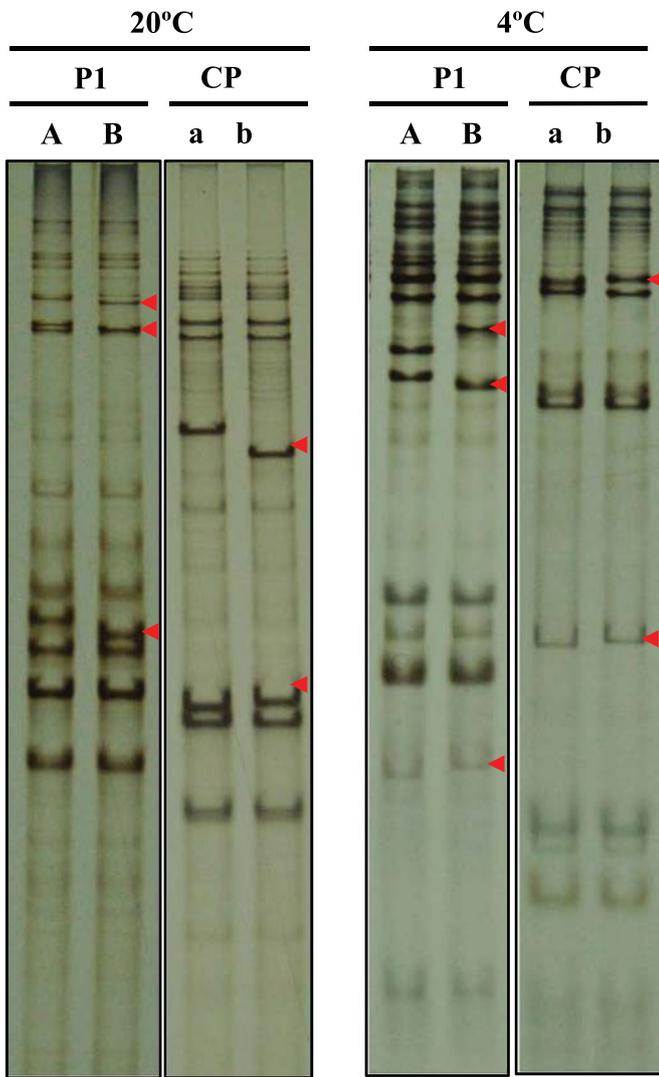
Fig. 2. Representative single-strand conformation polymorphism (SSCP) analysis results for TriMV coat protein (CP) and protein 1 (P1) regions. Shown are SSCP patterns (phenotypes) of 'A' or 'a' of the original (founding) inoculum and the observed new phenotype 'B' or 'b' in passage 9. P1 PCR products were digested with *Ban* I, *Pst* I and *Pvu* II restriction endonucleases while CP PCR products were digested with *Dde* I prior to denaturation and electrophoresis on non-denaturing 10% polyacrylamide gels in TBE at 20 °C and 4 °C. Likewise, all SSCP patterns differing from the original phenotype 'A' or 'a' at one or both temperatures were assigned a unique letter designating a new phenotype.

Table 1
Phenotypes[a] and Gene Identity[b] values from SSCP pattern analysis of nine passage/replicate lineage populations from P1 and coat protein (CP) regions of TriMV.

Passage	Replicate I	Replicate II	Replicate III
P1: 9	A (18), B, C	A (15), D, E, F, G, H	I (17), J, K, L
	[0.805 ± 0.026]	**[0.553 ± 0.031]**	**[0.716 ± 0.029]**
18	A (18), M, N	A (16), O, P, Q, R	A (14), T, U, V, W, X, Y
	[0.805 ± 0.026]	**[0.632 ± 0.030]**	**[0.479 ± 0.030]**
24	A (16), Z (2), AA, BB	A (19), CC	A (19), DD
	[0.637 ± 0.029]	**[0.900 ± 0.020]**	**[0.900 ± 0.020]**
CP: 9	a (16), b, c, d, e	a (18), f, g	a (13), h, i, j, k, l, m, n
	[0.632 ± 0.030]	**[0.805 ± 0.026]**	**[0.411 ± 0.029]**
18	a (15), o, p, q, r, s	t (16), u, v, w, x	t (17), y (2), z
	[0.553 ± 0.031]	**[0.632 ± 0.030]**	**[0.721 ± 0.28]**
24	a (18), aa, bb	t (5), cc (4), dd, ee (8),	t (19), hh
	[0.805 ± 0.026]	ff, gg **[0.232 ± 0.014]**	**[0.900 ± 0.020]**

[a] Samples of 20 clones from P1 and CP genomic regions of the nine passage/replicate populations were screened by SSCP as described in the legend of Fig. 2. Letters were arbitrarily assigned to each distinct SSCP pattern (phenotype) followed by in parentheses are the number of times that pattern occurred. Pattern 'A' (P1) or 'a' (CP) are identical to those of the TriMV infectious clone used to establish the three replicate lineages.

[b] Sample gene identity values (bold numbers in brackets) are calculated as 1 − (sample heterozygosities) ± standard error (Nei, 1987, equations (8.4) and (8.12)). Gene identity is the probability that any two clones derived from the same population will have identical phenotypes.

Table 2
Cumulative binomial probability (P) that a particular SSCP pattern will be observed at least Y times out of 20 clones when that phenotype is present in the population at several levels of relative population frequencies.

Relative population frequency	$P(Y \geq 0)$	$P(Y \geq 1)$	$P(Y \geq 2)$	$P(Y \geq 5)$	$P(Y \geq 10)$	$P(Y \geq 15)$
1%	1.00	0.18	0.02	0.00	0.00	0.00
5%	1.00	0.64	0.26	0.00	0.00	0.00
10%	1.00	0.88	0.61	0.04	0.00	0.00
25%	1.00	1.00	0.98	0.59	0.01	0.00
50%	1.00	1.00	1.00	0.99	0.59	0.02
75%	1.00	1.00	1.00	1.00	1.00	0.62
90%	1.00	1.00	1.00	1.00	1.00	0.99
95%	1.00	1.00	1.00	1.00	1.00	1.00

present at low frequencies (< 1%) in the sampled populations. Samples with multiple clones with the same phenotype must have substantially higher population frequencies. Eight phenotypes (including the two founding phenotypes) were observed multiple times (Table 1). These ranged from twice to 19 times, suggesting their population frequencies ranged from 25% to greater than 95%.

These results suggest that the composition of both intra-plant and serially transmitted inter-host populations of TriMV have a large stochastic component. This best illustrated by following the fate of the founding phenotypes in the P1 and CP regions (Table 1). For the P1 region, phenotype 'A' was retained in replicate I populations across passages 9 and 18 with 18 clones each, and decreased slightly to 16 clones by passage 24 (not significant, $P=0.86$) (Table 1). Similarly no significant difference in phenotype 'A' frequencies was detected among the passage 9, 18, and 24 populations of replicate II with 15, 16, and 19 phenotype 'A' clones, respectively ($P=0.61$). Phenotype 'A' was missing at passage 9 of replicate III but later reappeared. The passage 18 population had

14 phenotype 'A' clones, and the passage 24 population contained 19 such clones, resulting in significant P values (< 0.05) for differences among phenotype 'A' frequencies for passage 9 compared to passages 18 or 24 (Table 1).

In contrast, the frequency of the founding phenotype 'a' of the CP region decreased over time for two of the replicates (Table 1). Replicate I retained similar phenotype 'a' frequencies across populations from passages 9, 18, and 24 with 16, 15, and 18 phenotype 'a' clones, respectively ($P \geq 0.7283$). However, replicates II and III had completely lost the 'a' phenotype by passage 18, resulting in a significant ($P < 0.001$) decline in the founding phenotype frequency (Table 1).

The most striking result of the phenotypic analysis was clear evidence of parallel evolution in the CP region. A shift from phenotype 'a' to phenotype 't' occurred in both replicates II and III (Table 1). Moreover, this new phenotype was present at non-trivial frequencies. Replicate II had 18 phenotype 'a' clones (90%) at passage 9 but none were observed in samples from passages 18 and 24. There were 16 (80%) and 5 (25%) phenotype 't' clones, respectively, at the latter two passages. Similarly, replicate III had 13 phenotype 'a' clones at passage 9 but were apparently replaced by 17 (85%) and 19 (95%) phenotype 't' clones at passages 18 and 24, respectively (Table 1). These results strongly suggest that phenotype 't' has a selective advantage over phenotype 'a' in this experimental setting. These results also underscore the previous

A

Passage/ Replicate	334 C	340 C	345 U	348 U	403 A	424 C	454 A	458 U	576 C	625 U	655 C	723/724 +	726/727 +	836 A	850 G	918 G	931 G	953 C	957 U	960 G	968 U	993 A	995 C	1023 C	1048 U	1052 G	1063 C	1071 G	1139 A	1201 U	1319 A	1364 G	1421 A	1448 C	1503 G	1537 A	1547 U	1556 G	1564 U	1744 U	1762 C	1842 U
												5'-UTR																P1															
Passage 9 / I	.	.	.	.	.	.	.	U	.	.	.			G	.	.	.	.	.	.	.	.	.	U	.	.	.	.	.	.	.	.	.	.	.	.	.	.	.	.	.	.
Passage 9 / II	.	.	.	.	.	U	.	.	.	C	.			.	.	.	.	A	.	A	.	.	.	.	.	.	.	.	.	.	G	.	.	.	.	.	.	.	.	.	.	U
Passage 9 / III	.	.	C	.	.	.	.	.	.	.	.	U/C (20)[a,b,c]	U(20)[a,c]	.	U	.	.	.	.	.	.	.	.	.	.	A	.	.	.	.	.	.	.	.	.	.	.	.	.	.	.	.
Passage 18 / I	.	.	.	.	.	.	.	C	.	.	.			.	.	.	.	.	.	.	.	.	.	.	.	.	.	.	.	.	.	.	.	.	.	.	.	G	.	.	.	.
Passage 18 / II	U	.	.	.	.	U	.	.	.	.	.			.	.	A	.	.	.	.	.	.	.	.	U	.	.	.	U	.	.	G	A	.	A	.	.	.	.	.	.	.
Passage 18 / III	.	U	.	G[d]	.	.	.	.	.	U(2)[a]	.			.	.	.	.	.	.	.	.	.	.	C	.	.	U	.	.	A	C	.	.	U	.	G	.	.	.	C	.	.	.
Passage 24 / I	.	.	.	.	.	.	.	.	.	.	.			.	.	.	.	.	.	.	.	.	.	.	.	.	C	.	.	.	.	.	.	A	.	.	A	C(4)	.	.	.
Passage 24 / II	.	.	.	.	.	.	.	.	.	U[b]	.			.	.	.	.	.	.	.	.	.	.	C	.	.	.	.	.	.	.	.	.	.	.	.	.	.	.	.	.	.
Passage 24 / III	.	.	.	.	.	.	.	.	.	.	.			.	.	.	.	.	.	.	.	.	.	U	.	.	.	.	.	.	.	.	.	.	.	.	.	.	.	.	.	G

B

Passage/Replicate	850 Lys	918 Ser	953 Pro	957 Met	960 Gly	968 Phe	993 Lys	995 Pro	1023 Thr	1052 Ala	1071 Arg	1139 Arg	1319 Asn	1364 Val	1421 Lys	1448 Gln	1503 Arg	1537 Ile	1547 Phe	1556 Val	1842 Leu
Passage 9 / I	.	.	.	.	.	.	Met	.	.	.	.	.	.	.	.	.	.	.	.	.	.
Passage 9 / II	.	.	.	.	Asp	.	.	.	.	.	.	Gly	.	.	.	.	.	.	.	.	.
Passage 9 / III	Asn	.	Ser	.	.	.	.	.	.	Thr	.	.	.	.	.	.	.	.	.	.	.
Passage 18 / I	.	.	.	.	.	.	.	.	.	.	.	.	.	.	.	.	.	.	Val	.	.
Passage 18 / II	.	Asn	.	.	.	.	.	Ser	.	.	.	.	Asp	Ile	.	Lys	.	.	.	.	.
Passage 18 / III	.	.	.	.	.	Leu	.	.	Ile	.	His	.	.	.	Stop[e]	.	Met	.	.	.	.
Passage 24 / I	.	.	.	.	.	.	.	.	.	.	.	.	.	.	.	.	Lys	.	.	Ile	.
Passage 24 / II	.	.	.	Thr	.	.	.	.	.	.	.	.	.	.	.	.	.	.	.	.	.
Passage 24 / III	.	.	.	.	.	.	.	Ser	.	.	.	.	.	.	.	.	.	.	.	.	Trp

Fig. 3. Nucleotide mutations or insertions/deletions and their frequencies detected within the TriMV P1 region in three replicates at passage 9, 18, and 24. (A) Presented are nucleotide mutations within a portion of the 5'UTR (nts 301–739) and the P1 cistron. [a]Number of clones containing the same mutation are given in parentheses; [b]Nucleotide insertion; [c]Mutation fixed in the population; and [d] Nucleotide deletion. (B) Presented are amino acid variations with in the P1 cistron. Nucleotide mutations that did not change the amino acid are not indicated. [e]Predicted lethal mutation.

conclusion that replicate populations are highly variable; at passage 24, replicate II had the lowest observed gene identity (0.232) while replicate III had the highest (0.900) (Table 1).

2.2. Genotypic analysis of cDNA clones

The P1 and CP phenotypes listed in Table 1 were further characterized by nucleotide sequencing. The sequences of phenotype 'A' and 'a' clones from available replicate passages (one clone per replicate/passage) were confirmed to have the same sequences as the initial infectious cDNA clone. Sequences of all clones with variant SSCP phenotype profiles (Table 1) were experimentally determined. P1 clones differed from each other by an average of 3.1 nt, while CP clones averaged 2.9 nt differences. Both singleton (mutations that occur only once) and non-singleton mutations (those that occur multiple times) were identified within the two data sets (Figs. 3 and 4).

Thirty-nine singleton and five non-singleton substitutions were found in the P1 region (Fig. 3A). Insertions and nucleotide substitutions occurred at several places in the 5'UTR but there is no reason to expect that these would disrupt translation of the open reading frame. Nine mutations, three synonymous and four non-synonymous substitutions in the P1 cistron and two substitutions in the 5'UTR, were found in replicate I of all three passages (Fig. 3A, B). In passage 24 of replicate I, a synonymous substitution of U_{1564} for C within a histidine codon was detected in four clones. A total of 16 mutations, five in the 5'UTR and eight non-synonymous and three synonymous substitutions in P1 cistron, were found over the three time points within replicate II (Fig. 3). The largest number of mutations was detected in replicate III. Seven mutations were found in the 5'UTR, and ten non-synonymous and two synonymous mutations were found in the P1 cistron. Passage 9 of replicate III had three fixed substitutions. Two were insertions of U and C between nucleotide positions 726 and 727 in the 5'UTR. Additionally, there was a non-synonymous mutation ($G_{850} \rightarrow U$) resulting in an amino acid change from lysine to asparagine (Fig. 3). In passage 18 of replicate III, a substitution of $A_{1421} \rightarrow U$ created a stop codon which likely would be lethal (Fig. 3A and B).

The CP region contained nine non-singleton and 35 singleton substitutions (Fig. 4). Substitutions arose throughout the entire CP region with no apparent regional bias. Thirteen substitutions were found within the CP region from all three passages of replicate I, of these ten were non-synonymous and three were synonymous (Fig. 4). A non-synonymous mutation at nucleotide position 9423 altered amino acid lysine to arginine (Fig. 4B). It was present in all three passages of replicate I, indicating an appreciable frequency before passage 9. Substitution of $C_{9917} \rightarrow U$ in passage 9 of replicate I resulted in change of amino acid arginine to a stop codon, which is likely lethal (Fig. 4A and B).

A

Passage/Replicate	9100 G	9106 C	9209 U	9222 A	9241 A	9315 G	9326 G	9328 U	9409 C	9423 A	9429 C	9448 C	9478 G	9485 U	9489 G	9504 C	9506 G	9537 C	9539 U	9550 C	9591 C	9630 U	9634 U	9651 C	9790 C	9817 G	9818 C	9822 A	9835 U	9848 G	9849 U	9873 A	9892 G	9917 C	9927 U	9954 C	10005 C	10009 U
	NIb		CP																																			
Passage 9 / I	.	.	.	.	.	.	.	.	.	G (4)[a]	.	.	.	.	.	.	A	.	.	.	.	.	.	U	.	U	.	.	.	.	.	.	.	U	.	.	.	.
Passage 9 / II	.	.	.	.	.	A	.	.	.	.	.	.	.	.	.	.	.	.	.	.	.	C	.	.	.	.	.	.	.	.	.	.	.	.	.	.	.	.
Passage 9 / III	.	.	A	U	.	.	.	A	.	.	U	U	.	.	.	.	.	.	.	.	C	.	.	.	.	.	.	.	.	A	C	G	.	.	.	.	.	A
Passage 18 / I	A	A	.	.	.	.	.	.	.	G (5)[a]	.	.	.	.	.	.	.	.	.	.	.	.	.	.	.	.	.	.	.	.	.	.	.	C	U	.	.	.
Passage 18 / II	.	.	.	.	.	.	.	.	.	.	.	U	A (20)[a,b]	.	.	U	.	.	.	.	.	.	.	.	.	-[c]	-[c]	G	.	.	.	.	A	.	.	.	.	.
Passage 18 / III	.	.	.	.	.	.	U	.	.	.	.	.	A (20)[a,b]	.	.	.	.	.	.	.	.	.	.	.	.	.	.	.	.	.	.	U	.	.	.	.	U	.
Passage 24 / I	.	.	.	.	.	.	.	.	.	G (2)[a]	.	.	.	.	.	.	.	.	.	.	C	C	.	.	.	.	.	.	.	.	.	.	.	.	.	.	.	.
Passage 24 / II	.	.	.	.	C	.	.	.	.	.	.	.	A (20)[a,b]	.	.	U	.	U	.	U (4)[a]	U (8)[a]	.	.	.	.	.	.	.	.	.	.	.	.	.	.	.	.	.
Passage 24 / III	.	.	.	.	.	.	.	.	.	.	.	.	A (20)[a,b]	C	.	.	.	.	.	.	.	.	.	.	.	.	.	.	.	.	.	.	.	.	.	.	.	.

B

Passage/Replicate	9106 Phe	9209 Ser	9222 Lys	9241 Thr	9315 Gly	9326 Asp	9328 Asp	9423 Lys	9429 Ala	9485 Phe	9489 Gly	9504 Ala	9506 Ala	9537 Ala	9539 Phe	9591 Ala	9630 Val	9651 Ala	9817 Pro	9818 His	9822 Asn	9848 Val	9849 Val	9873 Asp	9917 Arg	9927 Val	9954 Pro	10005 Thr	10009 Asn
	NIb	CP																											
Passage 9 / I	.	.	.	.	.	.	.	Arg	.	.	.	.	Thr	.	.	.	.	Val	.	.	.	.	.	.	Stop[d]	.	.	.	.
Passage 9 / II	.	.	.	.	Asp	.	.	.	.	.	.	.	.	.	.	.	.	.	.	.	.	.	.	.	.	.	.	.	.
Passage 9 / III	.	Thr	Met	.	.	.	Glu	.	Val	.	.	.	.	.	.	Leu	.	.	.	.	.	Thr	Thr	Gly	.	.	.	.	Lys
Passage 18 / I	Leu	.	.	.	.	.	.	Arg	.	.	.	.	.	.	.	.	.	.	.	.	.	.	.	.	Ala	Leu	.	.	.
Passage 18 / II	.	.	.	.	.	.	.	.	.	.	.	Val	.	.	.	.	.	.	-[d]	-[d]	Ser	.	.	.	.	.	.	.	.
Passage 18 / III	.	.	.	.	.	Tyr	.	.	.	.	.	.	.	.	.	.	.	.	.	.	.	.	.	.	.	.	.	Met	.
Passage 24 / I	.	.	.	.	.	.	.	Arg	.	.	.	.	.	.	.	.	Ala	.	.	.	.	.	.	.	.	.	.	.	.
Passage 24 / II	.	.	.	Pro	.	.	.	.	.	Val	.	.	Val	.	Val	.	.	.	.	.	.	.	.	.	.	.	.	.	.
Passage 24 / III	.	.	.	.	.	.	.	.	.	Leu	.	.	.	.	.	.	.	.	.	.	.	.	.	.	.	.	.	.	.

Fig. 4. Nucleotide mutations or deletions and their frequencies detected in the TriMV CP region in three replicates at passage 9, 18, and 24. (A) Presented are nucleotide mutation within the CP region containing part of the NIb cistron (nts 9001–9193) followed by the complete CP cistron (nt 9194–10,078). [a]Number of clones containing the same mutation are given in parentheses; [b]Mutation fixed in the population; and [c]Nucleotide deletion. (B) Presented are amino acid variations within the CP region. Nucleotide mutations that did not change the amino acid are not indicated. [d]Predicted lethal mutation.

A total of 15 mutations, 9 non-synonymous and 6 synonymous, were found in all three passages of replicate II (Fig. 4). Two deletions were detected in passage 18 at nucleotide positions 9817 and 9818, which resulted in a lethal frameshift mutation. In replicate III, 16 substitutions, 12 non-synonymous and 4 synonymous, were found. Notably, a fixed synonymous mutation ($G_{9478} \rightarrow A$) within a leucine codon was found in all sequenced clones of passages 18 and 24 of replicates II and III (Fig. 4; listed in Table 1 as phenotypes t, u, v, w, x, y, z, cc, dd, ee, ff, gg, and hh) provided evidence for parallel evolution in the TriMV CP cistron.

2.3. Mutation frequencies of TriMV within the P1 and CP regions

A summary of number of nucleotide substitutions observed in the TriMV P1 and CP regions, presented in Table 3. Replicates I, II, and III for each passage were pooled to determine the overall mutation frequency (i.e. the total number of mutations observed divided by the total number of bases sequenced) per passage. Mutations arising multiple times within a replicate/passage combination were counted only once for determining the total number of polymorphisms. The mutation frequency observed in the P1 region was 0.765×10^{-4}/nt (Table 3) at passage 9. By passage 18, the mutation frequency was increased to 1.419×10^{-4}/nt. The viral mutation frequency could not be determined for passage 24 because the observed substitution rate is not greater than the estimated RT-PCR error rate. Therefore, it was not possible to distinguish whether the eight polymorphisms observed in passage 24 were true polymorphisms or artifacts of RT-PCR. The average frequency for P1 was 0.748×10^{-4}/nt. Slightly higher corrected mutation frequencies were found in the CP region. The mutation frequencies observed at passages 9, 18 and 24 were 1.949×10^{-4}/

Table 3

Nucleotide polymorphisms found within the TriMV P1 and CP regions after 9, 18, and 24 passages.

PCR product	Passage	No. of polymorphic sites/nt sequenced	Mutation frequency (i.e. no. of mutations observed/nt sequenced)[a]	Adjusted[b] total mutation frequency	Mutation frequency/passage
P1	9	15/91,740	1.635×10^{-4}	0.765×10^{-4}	0.085×10^{-4}
	18	21/91,740	2.289×10^{-4}	1.419×10^{-4}	0.079×10^{-4}
	24	8/91,740	0.870×10^{-4}	0	0
CP	9	17/60,300	2.819×10^{-4}	1.949×10^{-4}	0.217×10^{-4}
	18	16/60,300	2.653×10^{-4}	1.783×10^{-4}	0.099×10^{-4}
	24	11/60,300	1.824×10^{-4}	0.954×10^{-4}	0.040×10^{-4}

[a] No significant difference using a Two-Way ANOVA ($P < 0.05$).

[b] Sporadic changes attributed to combined error (0.870×10^{-4}/nt) due to RT (0.588×10^{-4}/nt) plus observed error rate for *Pfu* II Ultra DNA polymerase (0.282×10^{-4}/nt) were subtracted to yield corrected mutation frequencies/nucleotide.

nt, 1.783×10^{-4}/nt and 0.954×10^{-4}/nt, respectively, for an average value of 1.562×10^{-4}/nt (Table 3). Nevertheless, differences in mutation frequencies among passages or between coding regions were not statistically significant.

3. Discussion

3.1. Populations resulting from serial transfer of progeny virus from an infectious cDNA clone of TriMV are diverse

Both phenotypic and genotypic compositions within the P1 and CP regions were largely random among replicate passaged populations (Table 1; Figs. 3 and 4). SSCP and nucleotide sequence analyses both provided useful information regarding the stochastic nature of genetic diversity among these populations, suggesting that genetic drift is the driving evolutionary process involved. Changes within the P1 and CP regions of TriMV were measured during serial passages at a high multiplicity of infection. It is clear from these results that TriMV populations are dynamic, with new genotypes arising, gaining predominance, losing predominance to other sequences, or serving as the basis for accumulation of further alterations. TriMV population variation was dominated by transient singletons within both P1 and CP regions. Thus genetic drift seems to be a primary factor influencing TriMV population structure and dynamics. This result is consistent with the findings of previous studies of other plant viruses (Choi et al., 2001; Cuevas et al., 2015; Dunham et al., 2014; Elena et al., 2008; French and Stenger, 2005; Hall et al., 2001a,b; Li and Roossinck, 2004; Sacristán et al., 2003; Simmons et al., 2011, 2012). Most transient mutants are likely due to a linear mode of viral replication resulting in the independent production of many singleton mutations.

There was one non-synonymous mutation of $A_{9423} \rightarrow G$ at the N-terminus of the CP cistron resulting in an amino acid change from arginine to lysine that was present in all passages of replicate I. It made up 20% of the population at passage 9, 25% at passage 18, and 10% at passage 24 (Fig. 4A). Assuming a binomial distribution, its expected frequency in each population was 0.2 ± 0.11, 0.25 ± 0.10, and 0.1 ± 0.09, respectively. This suggests that this substitution was neutral, or nearly so, and was able to coexist with the parental CP genotype.

3.2. Evidence for selection in TriMV

In the P1 region, phenotype 'I' was present at a high frequency in the passage 9 population of replicate III but it was replaced by the founding type 'A' in the passage 18 and 24 populations (Table 1). This shift towards the founding genotype 'A' likely is an example of negative selection, perhaps driven by the importance of TriMV P1 in suppressing host RNA silencing (Tatineni et al., 2012). Indeed, genotype 'A' was present at high frequencies in all other P1 populations.

Most strikingly, a synonymous mutation of $G_{9478} \rightarrow A$ in the CP cistron was found in both replicates II and III at passages 18 and 24 (Fig. 4). Not only was it present in two independent lineages but it occurred in all 20 clones sampled from each of all four populations, meaning that it was a completely fixed substitution. Parallel or convergent evolution in viruses was first described for a bacteriophage (Bull et al., 1997). Several examples of parallel evolution have been noted previously for plant viruses following adaptation to alternative hosts, e.g Turnip mosaic virus (Tan et al., 2005), Plum pox virus (Wallis et al., 2007) and Tobacco etch virus (Hillung et al., 2014). However, as far as we know it is the first example of parallel evolution in a plant virus following serial passage in its natural host. Furthermore, it is a remarkable

example of selection at the RNA sequence level. The reason for the apparent strong selective advantage of the $G_{9478} \rightarrow A$ substitution is unclear. This substitution is not present in any of 50 field-collected TriMV isolates sequenced to date (Fellers et al., 2009; French, unpublished; Fuentes-Bueno et al., 2011; Seifers et al., 2013; Tatineni et al., 2009). The RNA region surrounding this silent substitution (nts 9228–9728) was subjected to secondary structure prediction analysis using mfold (version 2.3) energies. Sequence with G_{9478} was predicted to be within a stem structure while sequence with A_{9478} was part of a loop (data not shown). However, significance of these secondary structures in virus biology is unknown.

The life history of an experimental virus population following serial passage differs from the life history of the same virus in its native setting. In the experiments described here there are a number of obvious differences. The wheat variety 'Tomahawk' is not widely cultivated at present. Field transmission of TriMV is solely by means of its mite vector, and the importance of alternative hosts in the life history of TriMV is unknown. Regardless of mechanism it is worth noting that despite low effective population sizes resulting from cell-to-cell movement, which favors genetic drift, Miyashita and colleagues (Miyashita and Kishino, 2010; Miyashita et al., 2015) have shown that selection for a favored genotype can quickly occur.

3.3. Mutation frequency per nucleotide of TriMV compared to other plant viruses

The mutation frequency identified within the P1 and CP regions of TriMV (Table 3) is low compared to those of other potyviruses. The mutation frequency in the CP of WSMV after nine serial passages in wheat was 5.8×10^{-4}/nt (French and Stenger, 2005; Hall et al., 2001b). While using the same methodology, we observed that the mutation frequency of TriMV CP was 1.95×10^{-4}/nt. Zucchini yellow mosaic virus (ZYMV) had a mutation frequency of 8.7×10^{-4}/nt over 1, 2 and 3 passages (Simmons et al., 2011). Mutation frequencies have also been determined for other plant viruses. For example, mutation frequencies for Tobacco mosaic virus and Cucumber mosaic virus were estimated to be 7.0×10^{-4}/nt and 9.0×10^{-4}/nt, respectively after ten passages (Schneider and Roossinck, 2000).

Estimation of actual mutation or error rates of plant viruses is technically difficult. Determining the degree to which genetic selection affects observed viral mutation frequencies is generally not possible (Combe and Sanjuán, 2014). Moreover, for plant RNA viruses, intrinsic error rates cannot be disentangled from reverse transcriptase error rates (Roberts et al., 1988, 1989; Menéndez-Arias 2009). However, we note that making the reasonable assumption that RNA virus replication is mainly linear (French and Stenger, 2003; García-Villada and Drake, 2012; Sanjuán et al., 2010; Sardanyés and Elena, 2011) mutation frequencies should closely fit a Poisson distribution. Thus, the null class or P(0) method (García-Villada and Drake, 2012; Luria, 1951; Luria and Delbruck, 1943) can be used to calculate experimental mutation rates from the expression $P(0) = e^{-M}$ where $P(0)$ is the proportion of clones without any mutations and M is the number of mutational events in a sample. If the total number of viral genomes in a sample (N) is known then the mutation rate per replication event is equal to M/N. Accordingly, the genetic data presented here for TriMV and parallel genetic data for WSMV provided by Hall et al. (2001b) can be combined with quantitative real-time PCR data for both viruses (Tatineni et al., 2010) to provide an approximate comparison of their respective mutation rates. Importantly, these two studies employed the same experimental host and similar procedures. Average $P(0)$ for TriMV at passage 9 was 16/20, hence $M_{TriMV} = 0.22$, and $P(0)$ for WSMV at passage 9 was 8/20

($M_{WSMV}=0.92$). Virion numbers were $10^{5.35}$ per sample for TriMV and $10^{5.1}$ per sample for WSMV (Tatineni et al., 2010). Therefore, the calculated mutation rate (M/N) for TriMV is proportional to 1×10^{-6} per CP region and that of WSMV is proportional to 7.2×10^{-6}. Thus, after normalization for different CP region target sizes (1005 nt for TriMV and 1371 nt for WSMV), the mutation rate of TriMV appears to be 5.3-fold lower than that of WSMV. Collectively, these results indicate that TriMV evolves slowly after serial passage, and future research is needed to determine the mechanistic basis for this observation.

4. Materials and methods

4.1. Inoculation of passages

An infectious cDNA clone of TriMV Nebraska isolate (Tatineni et al., 2015) was used to synthesize *in vitro* transcripts using SP6 MEGAscript high yield transcription kit (Life Technologies, Grand Island, NY). Wheat cv. Tomahawk seedlings were inoculated with *in vitro* transcripts at the single leaf stage. One pot of wheat seedlings was inoculated with sterile water as a control. Three wheat plants infected with *in vitro* transcripts were randomly selected to initiate serial transmission replicates I, II, and III for 24 serial passages at 14-day intervals. For each replicated lineage at each passage, one systemically infected symptomatic leaf was collected at 14 days post-inoculation (dpi) to prepare the crude extract at 10^{-1} dilution in sterile water. This extract was used to inoculate 16–18 wheat seedlings at the two-leaf stage. Plants were maintained in a greenhouse at 20 to 26 °C.

4.2. RT-PCR and cloning

At 14 dpi, two upper symptomatic leaves were collected from each replicate at passages 9, 12, 15, 18, 21, and 24 for total RNA extraction as described in McNeil et al. (1996). Two µl of total RNA was used for reverse transcription with reverse primers specific to P1 or CP region (see below) using *Avian myeloblastosis virus* (AMV) reverse transcriptase (Roche, Indianapolis, IN) in a 10 µl volume. Two PCR reactions were performed on each replicate sample for passages 9, 18, and 24 targeting the P1 or CP region (Fig. 1) using high fidelity *Pfu* II Ultra polymerase (Agilent, Santa Clara, CA). The P1 and CP regions were amplified using oligonucleotides Tr-72 (corresponding to nt 301–318) and Tr-76 (complementary to nt 1888–1860), and Tr-89 (corresponding to nt 9001–9019) and Tr-100 (complementary to nt 10,078–10,048), respectively. One µl of cDNA was used for PCR in 25 µl reaction volumes with the P1 or CP region specific primers. The PCR program consisted of 95 °C for 2 min, followed by 10 cycles at 95 °C for 30 s, 48 °C for 30 s and 72 °C for 2 min. The annealing temperature was increased to 56 °C for the remaining 30 cycles, for a total of 40 cycles.

A Zero Blunt TOPO PCR Cloning Kit (Invitrogen, Carlsbad, CA) was used to clone PCR products. Plasmid DNAs that contain either the P1 or CP region were diluted to 1:500 in sterile water, and re-amplified by PCR using the previously described primers and PCR conditions.

4.3. SSCP analysis

SSCP has been utilized to identify single nucleotide differences at various points in time from the initial founding sequence (Gasser et al., 2006; Goszczynski, 2007; Hall et al., 2001b; Kong et al., 2003; Orita et al., 1989; Pawlotsky et al., 1998; Rubio et al., 1996; Welsh et al., 1997). The electrophoretic mobility of a single-stranded DNA molecule in non-denaturing gels is highly dependent on its size and sequence-dependent structure (Gasser et al., 2006; Orita et al., 1989), and the accuracy of SSCP to detect single nucleotide polymorphisms improves to ~98% when two gels are electrophoresed at different temperatures (Welsh et al., 1997). Thus, SSCP analysis was performed at 20 °C and 4 °C and PCR products with SSCP patterns identical to those of the founding inoculum were considered to be free of mutations. Nevertheless, a few (~2%) true genetic variants may have been missed.

SSCP analysis was performed on 20 positive clones from passages 9, 18, and 24 from each replicate lineage (I, II, and III) for both the P1 and CP regions (Fig. 1). The final PCR products were digested with appropriate restriction enzymes to digest into ~200–500 bp fragments required for SSCP analysis (Fig. 2) (Orita et al., 1989). Digested samples were prepared for SSCP as described in Hall et al. (2001b). DNA fragments were separated on 10% Tris-Borate-EDTA polyacrylamide gels (Life Technologies) in 1X TBE buffer at 20 °C and 4 °C for 16.5 and 15.5 h, respectively. Silver staining of SSCP gels was performed using a GE Healthcare DNA Silver Staining Kit PlusOne (GE Healthcare, Waukesha, WI). Samples displaying SSCP patterns dissimilar from the positive control (pTriMV) were prepared for sequencing.

4.4. Error rate of reverse transcriptase and PCR

The error rate of the PCR system employed in this investigation was assessed as described in Hall et al. (2001b). Briefly, the P1 and CP regions were amplified from the TriMV infectious cDNA clone (Tatineni et al., 2015) with the same primer sets described above. Fourteen clones each of the P1 and CP regions were then sequenced. Nucleotide mutations identified within the P1 and CP region were attributed to DNA polymerase errors introduced during PCR. The AMV reverse transcriptase (RT) error rate has been previously identified as one error per 17,000 nucleotides transcribed (0.588×10^{-4}/nt) (Roberts et al., 1988, 1989; Menéndez-Arias, 2009). Sporadic changes attributed to combined error (0.870×10^{-4}/nt) due to RT (0.588×10^{-4}/nt) plus observed error rate for *Pfu* II Ultra DNA polymerase (0.282×10^{-4}/nt) were subtracted from mutation rates of P1 and CP regions to obtain corrected mutation frequencies/nucleotide.

4.5. Nucleotide sequencing and analyses

Plasmids were treated with 2 ng RNase A for 20 min at 37 °C, followed by phenol:chloroform extraction and ethanol precipitation, and were sent to the Interdisciplinary Center for Biotechnology Research, University of Florida, for nucleotide sequencing. Sequence results were assembled using Sequencher 4.6 (Gene Codes Corporation, Ann Arbor, MI) and analyzed using DnaSP v5 (Librado and Rozas, 2009). RNA secondary structure analysis was performed using mfold (version 2.3 energies) (Zuker, 2003).

Gene identity values were calculated within each replicate and passage as 1 − (sample heterozygosities) ± standard error (Nei, 1987, equations 8.4 and 8.12). Statistical analysis was completed using SAS version 9.2 (SAS Institute Inc.). Two-way Analysis of Variance (ANOVA) was used to compare variation within and between passages, replicates, and/or regions (P1 and CP).

References

Acosta-Leal, R., Duffy, S., Xiong, Z., Hammond, R.W., Elena, S.F., 2011. Advances in plant virus evolution: translating evolutionary insights into better disease management. Phytopathology 101, 1136–1148.

Albiach-Martí, M.R., Mawassi, M., Gowda, S., Satyanarayana, T., Hilf, M.E., Shanker, S., Almira, E.C., Vives, M.C., Lopez, C., Guerri, J., Flores, R., Moreno, P., Garnsey, S. M., Dawson, W.O., 2000. Sequences of *Citrus tristeza virus* separated in time and space are essentially identical. J. Virol. 74, 6856–6865.

Bull, J.J., Badgett, M.R., Wichman, H.A., Huelsenbeck, J.P., Hillis, D.M., Gulati, A., Ho, C., Molineux, I.J., 1997. Exceptional convergent evolution in a virus. Genetics 147, 1497–1507.

Burrows, M., Franc, G., Rush, C., Blunt, T., Ito, D., Kinzer, K., Olson, J., O'Mara, J., Price, J., Tande, C., Ziems, A., Stack, J., 2009. Occurrence of viruses in wheat in the great plains region, 2008. Plant Health Prog. http://dx.doi.org/10.1094/PHP − 2009 − 0706 − 01-RS

Byamukama, E., Seifers, D.L., Hein, G.L., De Wolf, E., Tisserat, N.A., Langham, M.A.C., Osborne, L.E., Timmerman, A., 2013. Occurrence and distribution of *Triticum mosaic virus* in the central great plains. Plant Dis. 97, 21–29.

Choi, I.-R., Hall, J.S., Henry, M., Zhang, L., Hein, G.L., French, R., Stenger, D.C., 2001. Contributions of genetic drift and negative selection on the evolution of three strains of *Wheat streak mosaic tritimovirus*. Arch. Virol. 146, 619–628.

Combe, M., Sanjuán, R., 2014. Variability in the mutation rates of RNA viruses. Future Virol. 9, 605–615.

Cuevas, J.M., Willemsen, A., Hillung, J., Zwart, M.P., Elena, S.F., 2015. Temporal dynamics of intra-host molecular evolution for a plant RNA virus. Mol. Biol. Evol. 32, 1132–1147.

Drake, J.W., 1993. Rates of spontaneous mutation among RNA viruses. Proc. Natl. Acad. Sci. USA 90, 4171–4175.

Drake, J.W., Holland, J.J., 1999. Mutation rates among RNA viruses. Proc. Natl. Acad. Sci. USA 96, 13910–13913.

Duffy, S., Shackelton, L.A., Holmes, E.C., 2008. Rates of evolutionary change in viruses: patterns and determinants. Nat. Rev. Genet. 9, 267–276.

Dunham, J.P., Simmons, H.E., Holmes, E.C., Stephenson, A.G., 2014. Analysis of viral (*Zucchini yellow mosaic virus*) genetic diversity during systemic movement through a *Cucurbita pepo* vine. Virus Res. 191, 172–179.

Elena, S.F., Agudelo-Romero, P., Carrasco, P., Codoñer, F.M., Martín, S., Torres-Barceló, C., Sanjuán, R., 2008. Experimental evolution of plant RNA viruses. Heredity 100, 478–483.

Fellers, J.P., Seifers, D., Ryba-White, M., Martin, T.J., 2009. The complete genome sequence of *Triticum mosaic virus*, a new wheat-infecting virus of the High Plains. Arch. Virol. 154, 1511–1515.

French, R., Stenger, D.C., 2003. Evolution of *Wheat streak mosaic virus*: dynamics of population growth within plants may explain limited variation. Annu. Rev. Phytopathol. 41, 199–214.

French, R., Stenger, D.C., 2005. Population structure within lineages of *Wheat streak mosaic virus* derived from a common founding event exhibits stochastic variation inconsistent with the deterministic quasi-species model. Virology 343, 179–189.

Fuentes-Bueno, I., Price, J.A., Rush, C.M., Seifers, D.L., Fellers, J.P., 2011. *Triticum mosaic virus* isolates in the Southern Great Plains. Plant Dis. 95, 1516–1519.

Gasser, R.B., Hu, M., Chilton, N.B., Campbell, B.E., Jex, A.J., Otranto, D., Cafarchia, C., Beveridge, I., Zhu, X., 2006. Single-strand conformation polymorphism (SSCP) for the analysis of genetic variation. Nat. Protoc. 1, 3121–3128.

García-Arenal, F., Fraile, A., Malpica, J.M., 2003. Variation and evolution of plant virus populations. Int. Microbiol. 6, 225–232.

García-Villada, L., Drake, J.W., 2012. The three faces of riboviral spontaneous mutation: Spectrum, mode of genome replication, and mutation rate. PLoS Genet. 8, e1002832.

Goszczynski, D.E., 2007. Single-strand conformation polymorphism (SSCP), cloning and sequencing reveal a close association between related molecular variants of *Grapevine virus A* (GVA) and Shiraz disease in South Africa. Plant Pathol. 56, 755–762.

Hall, J.S., French, R., Hein, G.L., Morris, T.J., Stenger, D.C., 2001a. Three distinct mechanisms facilitate genetic isolation of sympatric wheat streak mosaic virus lineages. Virology 282, 230–236.

Hall, J.S., French, R., Morris, T.J., Stenger, D.C., 2001b. Structure and temporal dynamics of populations within *Wheat streak mosaic virus* isolates. J. Virol. 75, 10231–10243.

Hillung, J., Cuevas, J.M., Valverde, S., Elena, S.F., 2014. Experimental evolution of an emerging plant virus in host genotypes that differ in their susceptibility to infection. Evolution 68, 2467–2480.

Holland, J., Spindler, K., Horodyski, F., Grabau, E., Nichol, S., VandePol, S., 1982. Rapid evolution of RNA genomes. Science 215, 1577–1585.

Kong, P., Hong, C., Richardson, P.A., Gallegly, M.E., 2003. Single-strand conformation polymorphism of ribosomal DNA for rapid species differentiation in genus *Phytophthora*. Fungal Genet. Biol. 39, 238–249.

Kong, P., Rubio, L., Polek, M., Falk, B.W., 2000. Population structure and genetic diversity within California *Citrus tristeza* virus (CTV) isolates. Virus Genes 21, 139–145.

Kurath, G., Palukaitis, P., 1990. Serial passage of infectious transcripts of a *Cucumber mosaic virus* satellite RNA clone results in sequence heterogeneity. Virology 176, 8–15.

Li, H., Roossinck, M.J., 2004. Genetic bottlenecks reduce population variation in an experimental RNA virus population. J. Virol. 78, 10582–10587.

Librado, P., Rozas, J., 2009. DnaSP v5: a software for comprehensive analysis of DNA polymorphism data. Bioinformatics 25, 1451–1452.

Luria, S.E., 1951. The frequency distribution of spontaneous bacteriophage mutants as evidence for the exponential rate of phage reproduction. Cold Spring Harbor Symp. Quant. Biol. 16, 463–470.

Luria, S.E., Delbruck, M., 1943. Mutations of bacteria from virus sensitivity to virus resistance. Genetics 28, 491–511.

McMechan, A.J., Tatineni, S., French, R., Hein, G.L., 2014. Differential transmission of *Triticum mosaic virus* by wheat curl mite populations collected in the Great Plains. Plant Dis. 98, 806–810.

McNeil, J.E., French, R., Hein, G.L., Baenziger, P.S., Eskridge, K.M., 1996. Characterization of genetic variability among natural populations of *Wheat streak mosaic virus*. Phytopathology 86, 1222–1227.

Menéndez-Arias, L., 2009. Mutation rates and intrinsic fidelity of retroviral reverse transcriptases. Viruses 1, 1137–1165. http://dx.doi.org/10.3390/v1031137.

Miyashita, S., Kishino, H., 2010. Estimate of the size of genetic bottlenecks in cell-to-cell movement of *Soil-borne wheat mosaic virus* and the possible role of the bottlenecks in speeding up selection of variations in *trans*-acting genes or elements. J. Virol. 84, 1828–1837.

Miyashita, S., Ishibashi, K., Kishino, H., Ishikawa, M., 2015. Viruses roll the dice: the stochastic behavior of viral genome molecules accelerates viral adaptation at the cell and tissue levels. PLoS Biol. 13, e1002094.

Nei, M., 1987. Molecular Evolutionary Genetics. Columbia University Press, New York, NY, USA.

Novella, I.S., Elena, S.F., Moya, A., Domingo, E., Holland, J.J., 1995. Size of genetic bottlenecks leading to virus fitness loss is determined by mean initial population fitness. J. Virol. 69, 2869–2872.

Orita, M., Iwahana, H., Kanazawa, H., Hayashi, K., 1989. Detection of polymorphisms of human DNA by gel electrophoresis as single-strand conformation polymorphisms. Proc. Natl. Acad. Sci. USA 86, 2766–2770.

Pawlotsky, J.M., Germanidis, G., Neumann, A.U., Pellerin, M., Frainais, P., Dhumeaux, D., 1998. Interferon resistance of *Hepatitis C Virus* genotype 1b: relationship to nonstructural 5A gene quasispecies mutations. J. Virol. 22, 2795–2805.

Roberts, J.D., Bebenek, K., Kunkel, T.A., 1988. The accuracy of reverse transcriptase from HIV-1. Sci. Rep. 242, 1171–1173.

Roberts, J.D., Preston, B.D., Johnston, L.A., Soni, A., Loeb, L.A., Kunkel, T.A., 1989. Fidelity of two retroviral reverse transcriptases during DNA-dependent DNA synthesis *in vitro*. Mol. Cell. Biol. 9, 469–476.

Rodriguez-Cerezo, E., Elena, S.F., Moya, A., Gacia-Arenal, F., 1991. High genetic stability in natural populations of the plant RNA virus *Tobacco mild green mosaic virus*. J Mol. Evol. 32, 328–332.

Rubio, L., Ayllón, M.A., Guerri, J., Pappu, H., Niblett, C., Moreno, P., 1996. Differentiation of *Citrus tristeza closterovirus* (CTV) isolates by single-strand conformation polymorphism analysis of the coat protein gene. Annu. Appl. Biol. 129, 479–489.

Sacristán, S., Malpica, J.M., Fraile, A., García-Arenal, F., 2003. Estimation of population bottlenecks during systemic movement of *Tobacco mosaic virus* in tobacco plants. J. Virol. 77, 9906–9911.

Safari, M., Roossinck, M.J., 2014. How does the genome structure and lifestyle of a virus affect its population variation? Curr. Opin. Virol. 9, 39–44.

Sanjuán, R., Nebot, M.R., Chirico, N., Mansky, L.M., Belshaw, R., 2010. Viral mutation rates. J. Virol. 84, 9733–9748.

Sardanyés, J., Elena, S.F., 2011. Quasispecies spatial models for RNA viruses with different replication modes and infection strategies. PLoS One 6, e24884.

Schneider, W.L., Roossinck, M.J., 2000. Evolutionarily related Sindbis-like plant viruses maintain different levels of population diversity in a common host. J. Virol. 74, 3130–3134.

Schneider, W.L., Roossinck, M.J., 2001. Genetic diversity in RNA virus quasispecies is controlled by host-virus interactions. J. Virol. 75, 6566–6571.

Seifers, D.L., Martin, T.J., Harvey, T.L., Fellers, J.P., Michaud, J.P., 2009. Identification of the wheat curl mite as the vector of *Triticum mosaic virus*. Plant Dis. 93, 25–29.

Seifers, D.L., Martin, T.J., Harvey, T.L., Fellers, J.P., Stack, J.P., Ryba-White, M., Haber, S., Krokhin, O., Spicer, V., Lovat, N., Yamchuk, A., Standing, K.G., 2008. *Triticum mosaic virus:* a new virus isolated from wheat in Kansas. Plant Dis. 92, 88–817.

Seifers, D.L., Tatineni, S., French, R., 2013. Variants of *Triticum mosaic virus* isolated from wheat in Colorado show divergent biological behavior. Plant Dis. 97, 903–911.

Simmons, H.E., Holmes, E.C., Stephenson, A.G., 2011. Rapid turnover of intra-host genetic diversity in *Zucchini yellow mosaic virus*. Virus Res. 155, 389–396.

Simmons, H.E., Dunham, J.P., Stack, J.C., Dickins, B.J., Pagan, I., Holmes, E.C., Stephenson, A.G., 2012. Deep sequencing reveals persistence of intra- and inter-host genetic diversity in natural and greenhouse populations of *Zucchini yellow mosaic virus*. J. Gen. Virol. 93, 1831–1840.

Slykhuis, J.T., 1955. *Aceria tulipae* keifer (*Acarina: Eriophyidae*) in relation to spread of *Wheat streak mosaic virus*. Phytopathology 45, 116–128.

Stenger, D.C., Hall, J.S., Choi, I.-R., French, R., 1998. Phylogenetic relationships within the family Potyviridae: wheat streak mosaic virus and Brome streak mosaic virus are not members of the genus *Rymovirus*. Phytopathology 88, 782–787.

Stenger, D.C., Seifers, D.L., French, R., 2002. Patterns of polymorphism in *Wheat streak mosaic virus*: sequence space explored by a clade of closely related viral genotypes rivals that between the most divergent strains. Virology 302, 58–70.

Tan, Z., Gibbs, A.J., Tomitaka, Y., Sánchez, F., Ponz, F., Ohshima, K., 2005. Mutations in *Turnip mosaic virus* genomes that have adapted *Raphanus sativus*. J. Gen. Virol. 86, 501–510.

Tatineni, S., Ziems, A.D., Hein, Wegulo, S.N., French, R., 2009. *Triticum mosaic virus:* a distinct member of the family *Potyviridae* with an unusually long leader sequence. Phytopathology 99, 943–950.

Tatineni, S., Graybosch, R.A., Hein, G.L., Wegulo, S.N., French, R., 2010. Wheat cultivar-specific disease synergism and alteration of virus accumulation during co-infection with *Wheat streak mosaic virus* and *Triticum mosaic virus.* Phytopathology 100, 230–238.

Tatineni, S., Qu, F., Li, R., Morris, J., French, R., 2012. *Triticum mosaic poacevirus* enlists P1 rather than HC-Pro to suppress RNA silencing mediated host defense. Virology 433, 104–115.

Tatineni, S., McMechan, A.J., Bartels, M., Hein, G.L., Graybosch, R.A., 2015. *In vitro* transcripts of wild-type and fluorescent protein-tagged *Triticum mosaic virus*

(Family *Potyviridae*) are biologically active in wheat. Phytopathology 105, 1496–1505.

Wallis, C., Stone, A.L., Sherman, D.J., Damsteegt, V.D., Gildow, F.E., Schneider, W.L., 2007. Identification of a mutation in the *Plum pox potyvirus* NIb gene associated with adaptation to pea (*Pisum sativum*). J. Gen. Virol. 88, 2839–2845.

Welsh, J.A., Castren, K., Vahakangas, K.H., 1997. Single-strand conformation polymorphism analysis to detect p53 mutations: characterization and development of controls. Clin. Chem. 43, 2251–2255.

Zuker, M., 2003. Mfold web server for nucleic acid folding and hybridization prediction. Nucleic Acids Res. 31, 3406–3415.